Wave-function mapping in multiple quantum wells using diluted magnetic semiconductors

S. Lee, M. Dobrowolska, and J. K. Furdyna
Department of Physics, University of Notre Dame, Notre Dame, Indiana 46556

L. R. Ram-Mohan
Departments of Physics and Electrical and Computer Engineering, Worcester Polytechnic Institute, Worcester, Massachusetts 01609
(Received 24 November 1998)

We have shown that in symmetric multiple quantum wells (QW's), wave functions of the lowest multiplet of states have rather surprising distributions, where some states are localized only in certain wells, and are *totally absent* in other wells. To demonstrate this experimentally, we have used magnetoabsorption measurements to map out the distribution of wave functions in multiple-quantum-well structures in which some layers consist of diluted magnetic semiconductors (DMS's). For this purpose we fabricated triple- and quintuple-QW systems consisting of $Zn_{1-x-y}Cd_xMn_ySe$ (DMS) and $Zn_{1-x}Cd_xSe$ (non-DMS) wells, separated by ZnSe (i.e., nonmagnetic) barriers. Transitions involving the lowest multiplet of states (i.e., the ground state split by interwell interactions) were clearly observed and well resolved at zero magnetic field. The wave-function behavior in multiple quantum wells of equal depth was investigated by observing the Zeeman splitting of the optical transitions at 30 K, where the Zeeman splitting of DMS band edges is small compared to the band offset, so that the wells remain in near-resonant condition. This in turn results in strong (resonant) interactions between the wells. The experiments clearly demonstrated that for certain states there are wells in which the probability of finding an electron or a hole vanishes. [S0163-1829(99)09215-2]

I. INTRODUCTION

Since the observation of coupling effects in multiple-quantum-well (QW) structures by Dingle, Gossard, and Wiegmann,[1] there has been considerable interest in this phenomenon due to its importance both in fundamental physics and in device applications.[2–8] However, in contrast to the attention given to the double-QW system,[9–13] structures comprised of more than two coupled wells (such as triple, quadruple, or quintuple wells) remain essentially unexplored due to their complex multiplicity of eigenstates—even though triple QW's have been shown to be superior to double QW's in the context of resonant tunneling.[14,15] Recently, coupling effects in symmetric triple QW's have been investigated using photoluminescence (PL) measurements[16] (where the only transition observed is that between the lowest levels of the ground-state triplet in the conduction and in the heavy-hole band). Information on interwell coupling in that system could be inferred from the dependence of the PL transition on well and barrier thicknesses.

A more interesting and fundamental feature of multiple QW's is the *wave-function distribution* of the coupled states. We will show in fact that some wells can act as *barriers* for particular eigenstates, whose wave function then vanishes in those wells, and consequently the state itself becomes insensitive to the properties of that well. This situation is quite different from the case of double QW's or superlattices, where the states are *always* localized in *all* wells. So far little attention has been given to such wave-function distributions in multiple QW's, either from a practical or from a fundamental viewpoint. A certain amount of literature exists on the wave functions of coupled states in the case of asymmetric triple QW's.[17,18] The wave functions in those systems are, however, physically not as revealing as in symmetric multiple QW's which we will be investigating in this paper.

We have undertaken to map out the wave-function distributions in these complex systems using as our tool the strong splitting of the band edges which occurs in diluted magnetic semiconductors (DMS's) in a magnetic field, as discussed in Sec. II B, and we have designed symmetric triple and quintuple quantum wells specifically for this purpose. Furthermore, rather than using photoluminescence, which is sensitive only to the lowest-energy levels of the ground-state multiplet of a coupled system, we will use optical absorption measurements, so that we can observe transitions associated with *all* states (excited multiplet states as well as the lowest state).

II. WAVE-FUNCTION DISTRIBUTION IN MULTIPLE QUANTUM WELLS

A. Eigenstate multiplets in symmetric coupled QW's

In quantum mechanical description, a particle in a system of coupled QW's is characterized by a wave function which is distributed throughout the entire structure. The spatial distribution of the wave function then provides a measure of the localization of the particle. In a single QW with finite barriers, it is quite clear that the wave functions of the lower-lying states have a stronger localization in the well because of smaller ''leakage'' into the barrier than that of the higher states. In multiple QW's coupled by reasonably narrow barriers, wave functions of the eigenstates in each well interact through the barrier with those of neighboring wells, and the energy levels are consequently split into multiplets. The simplest coupled system is the double quantum well (DQW). The interwell coupling in such a system has been studied in detail[19] by investigating the behavior of optical transition as the barrier width and/or height are systematically varied.

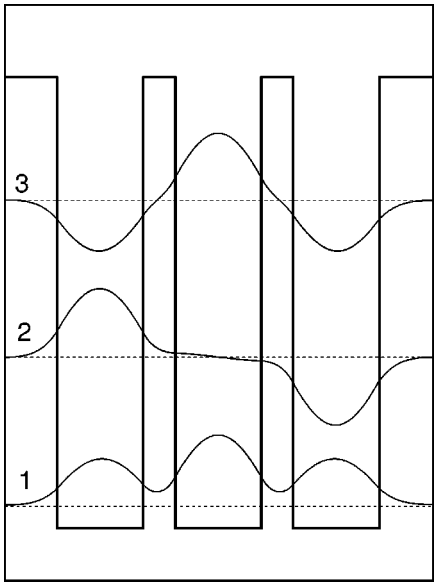

FIG. 1. Wave functions for the three lowest states in a symmetric triple-quantum-well system.

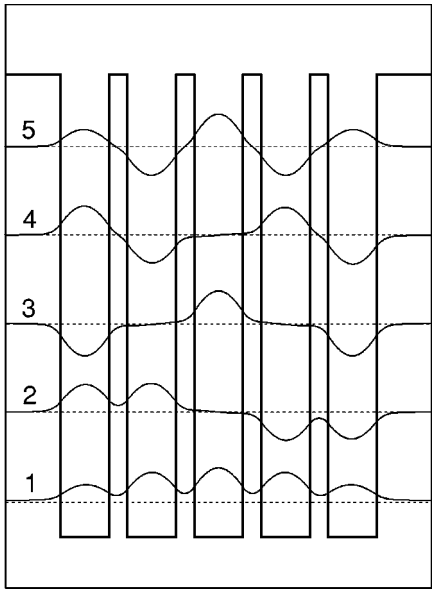

FIG. 2. Wave functions for the five lowest states in a symmetric quintuple-quantum-well system.

Here we select the specific cases of three and five coupled QW's, because they serve to illustrate new features in wave-function distribution of the coupled states, not present in the DQW. The wave functions of these multiple QW's are calculated using the $\mathbf{k}\cdot\mathbf{p}$ model and the ''finite element method.''[20] The versatility of the latter algorithm, and its suitability for investigating systems of this type, was discussed in Ref. 19. Since the structures considered here have more layers (i.e., more elements) than DQW's, a great amount of computing time would be required if all eight bands were to be taken into account, as was done for the DQW's. A one-band model does, however, provide a reasonably accurate picture, illustrating all the important trends, and we will adopt this simpler approach for dealing with multiple coupled wells in the present discussion. This approach has the added advantage of keeping the physics of the system clearly in evidence.

Figures 1 and 2 represent the wave functions of the lowest coupled states for the conduction band in symmetric triple and quintuple QW's, the picture being essentially the same for the valence band. In the case of the triple QW, our calculations show that the first and the third of the lowest triplet of states have some fraction of their wave functions in each of the wells. In the case of the second state, however, the wave function vanishes totally in the central well, representing in effect an ''electronic blind spot.'' This is quite surprising at first glance. Similarly, if we extend the analysis to the quintuple-well system, we find—as is seen in Fig. 2—that certain states (the second, the third, and the fourth) are localized in only some of wells, and are completely absent in others. Since the wave-function distributions such as those shown in Figs. 1 and 2 arise directly from interactions between states in different wells, a systematic investigation of such distributions—which can be done spectroscopically, as shown below—will significantly contribute to our understanding of the fundamental physics specific to multiple-QW structures.

B. Mapping of wave-function distribution in multiple QW's using DMS's

A variety of III-V semiconductor multiple-QW structures have been successfully used for exploring a number of dynamical phenomena, such as interwell tunneling and the effect of interwell coupling on the states of confined carriers.[21–23] However, the actual wave-function profile cannot normally be confirmed experimentally in these complex systems. Here the fabrication of II-VI-based multiple QW's involving DMS's does provide an opportunity to map wave-function distributions in a simple and elegant manner. The central idea is that, in structures consisting of alternating DMS and non-DMS layers, the Zeeman splitting of a given state will reflect its weighted probability distribution over the two media. In other words, the Zeeman splitting will be determined by how many localized magnetic moments the electron ''sees'' when it is in a particular state. If the wave function of the electron is strongly localized in the non-DMS layers, the splitting will be negligible; if it is strongly localized in the DMS layers, the splitting will be very large; etc. This technique has already been used to pinpoint the localization of above barrier states in superlattices[24–26] and in single barriers.[27] In the present study we will use the same idea as the tool for mapping wave-function distributions in multiple QW's.

For the multiple-QW structures used in this study, we have fabricated multilayer systems which consist of some magnetic and some nonmagnetic QW's, in all cases using nonmagnetic barriers. Inspection of the wave-function distribution shown in Fig. 1 suggests symmetric triple-QW structures in which DMS layers are used either for the center well or for the two side wells. It is easy to see from Fig. 1 that when only the center well is a DMS layer, the first and the third state—which are partially localized in that layer—will be strongly influenced by the magnetic field, while the second state—which is localized only in the side wells—will show negligible dependence on the field. On the other hand, in a system where the two side wells consist of DMS layers,

TABLE I. Calculated wave-function overlap for e_nh_n transitions in triple QW's.

e_1h_n	Overlap	e_2h_n	Overlap	e_3h_n	Overlap
e_1h_1	0.893	e_2h_1	0.001	e_3h_1	0.440
e_1h_2	0.002	e_2h_2	0.997	e_3h_2	0.002
e_1h_3	0.444	e_2h_3	0.003	e_3h_3	0.893

the second state will be affected by the magnetic field—in fact more so than the other states. Similarly, quintuple QW's can be conveniently studied by using DMS layers for the center well, or for wells 2 and 4, since some states have zero probability in those wells, as is clearly seen in Fig. 2. By observing the Zeeman splitting of optical transitions between specific states in systems fabricated in this way, we can determine in which layer (i.e., where in physical space) a given transition actually occurs.

Since such mapping is carried out by means of optical *interband* absorption, it will necessarily involve states in both the valence and the conduction bands. To facilitate further discussion, we will first identify transitions which will be of importance in this process, and we will define their designations. Transitions from the mth heavy-hole subband to the nth conduction subband will be designated e_nh_m; similarly, transitions from the mth light-hole subband to the nth electron subband will be designated as e_nl_m. Light-hole transitions are generally much weaker than those associated with the heavy holes because of the low density of states that characterizes the light-hole band. Furthermore, the Zeeman splitting of the e_nl_m transitions is about an order of magnitude smaller than that of e_nh_m. They are thus not particularly useful for wave-function mapping, which is the focus of this paper. We will therefore concern ourselves primarily with the e_nh_m transitions, originating from the heavy-hole band.

It is also necessary to identify the selection rules which govern the dominant e_nh_m transitions. In a single QW, selection rules are given by the simple relation $m=n$, which from now on we will write as $\Delta n=0$. In multiple QW's, selection rules are determined by the wave-function overlap,

$$\int \psi_i \psi_f^* dz,$$

where the ψ_f and ψ_i are the wave functions of the final state in the conduction band and the initial state in the valence band, respectively, and z is the axis parallel to the growth direction. The calculated overlap integrals for the transitions in triple QW's are given in Table I. It is easy to see that for transitions from a symmetric to an antisymmetric state (e.g., e_1h_2) the overlap integrals vanish, and these transitions are thus totally forbidden. Furthermore, the overlap integrals for transitions from one symmetric state to another symmetric state with $\Delta n\neq 0$ (e.g., e_1h_3), even if finite, are weaker than the $\Delta n=0$ transitions. So for any given multiple-QW system investigated here, the absorption spectrum will be dominated by e_nh_n transitions (e_1h_1, e_2h_2, e_3h_3, etc.). These transitions will thus be used in the mapping procedure.

III. EXPERIMENT

Symmetric triple-QW structures were fabricated using ZnSe for the barriers and the non-magnetic $Zn_{1-x}Cd_xSe$ for the wells. Cd concentration in well layers was chosen as $x\approx 0.2$, providing sufficient band offset in the heavy-hole band to confine all three eigenstates of the ground-state triplet. For Zeeman mapping of the wave-function distributions in such structures, however, we also need to use DMS layers for some of the wells. $Zn_{1-y}Mn_ySe$ cannot be used for that purpose, since it has approximately the same (or larger) band gap as ZnSe, depending on the value of y. Thus we have used a quaternary alloy $Zn_{1-x-y}Cd_xMn_ySe$, with $x\approx 0.2$ and $y\approx 0.04$, for the DMS wells. In that alloy, the chosen Mn ion concentration of $y\approx 0.04$ gives a similar energy gap in the DMS well as that of the $Zn_{1-x}Cd_xSe$ nonmagnetic wells. The well and barrier thicknesses were chosen to give sufficiently strong coupling between the wells, so that the e_nh_n transitions between different levels of the ground-state multiplet could be resolved. For triple QW's two complementary structures were fabricated, with the $Zn_{1-x-y}Cd_xMn_ySe$ layers used either for the center well (sample TQW1) or for the two side wells (TQW2), as suggested by earlier discussion.

The structures were grown by molecular beam epitaxy (MBE) on a 2-μm ZnSe buffer layer, deposited directly on GaAs(100) substrates. After depositing the triple QW's, the structures were capped by a 1-μm ZnSe protective layer. Similarly, two quintuple QW's were grown, with DMS layers used either for the central well (QQW1) or for the second and fourth wells (QQW2), and with similar dimensions and materials for the barriers and for the nonmagnetic and magnetic wells as those described above. Parameters for these multiple QW's are given in Table II, and the structures are schematically shown in Fig. 3, where the DMS and non-DMS wells are indicated as darkly and lightly shaded regions, respectively.

Since the band edge splitting shown by the $Zn_{1-x-y}Cd_xMn_ySe$ layer in a magnetic field will play a central role in the mapping of wave-function distributions in the multiple QW's described above, it is important to discuss at the outset the Zeeman splitting of the DMS layer itself in some detail. It was shown that the effective spin of the manganese ions, which determines the Zeeman splitting of DMS's, is practically independent of the host crystal[28] (i.e., it is essentially the same in $Zn_{1-y}Mn_ySe$, $Zn_{1-y}Mn_yTe$, or

TABLE II. Sample description.

Sample	Barrier	Non-DMS well	DMS well	L_w	L_b	x	y
TQW1	ZnSe	$Zn_{1-x}Cd_xSe$	$Zn_{1-x-y}Cd_xMn_ySe$	52 Å	20 Å	0.20	0.04
TQW2	ZnSe	$Zn_{1-x}Cd_xSe$	$Zn_{1-x-y}Cd_xMn_ySe$	38 Å	18 Å	0.20	0.04
QQW1	ZnSe	$Zn_{1-x}Cd_xSe$	$Zn_{1-x-y}Cd_xMn_ySe$	40 Å	20 Å	0.20	0.04
QQW2	ZnSe	$Zn_{1-x}Cd_xSe$	$Zn_{1-x-y}Cd_xMn_ySe$	40 Å	20 Å	0.21	0.04

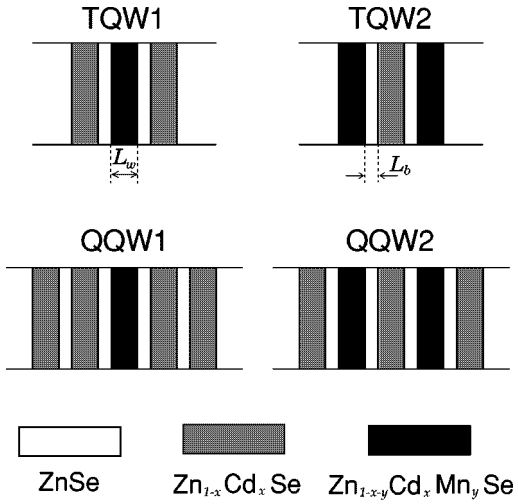

FIG. 3. Schematic diagrams for the symmetric multiple QW's (TQW1, TQW2, QQW1, and QQW2) consisting of $Zn_{1-x-y}Cd_xMn_ySe$ and $Zn_{1-x}Cd_xSe$ wells, with ZnSe barriers. Shaded regions indicate wells (dark color for $Zn_{1-x-y}Cd_xMn_ySe$ and light color for $Zn_{1-x}Cd_xSe$ wells), and unshaded regions are ZnSe barriers.

$Cd_{1-y}Mn_ySe$ for the same y). The Zeeman splitting in $Zn_{1-x-y}Cd_xMn_ySe$ layers with $y \approx 0.04$ used in this work will thus be very similar to that in $Zn_{1-y}Mn_ySe$ with $y \approx 0.04$. The Zeeman splitting of the band edge of $Zn_{1-y}Mn_ySe$, $y \approx 0.04$ for the conduction and the heavy-hole band determined experimentally in earlier studies[29] is shown as a function of magnetic field in Fig. 4. This variation indicates how the depth of DMS wells in the multiple-QW structures will change with field for the two spin orientations. Note the much larger Zeeman shift of the heavy-hole band, characteristic of II-VI-based DMS's.

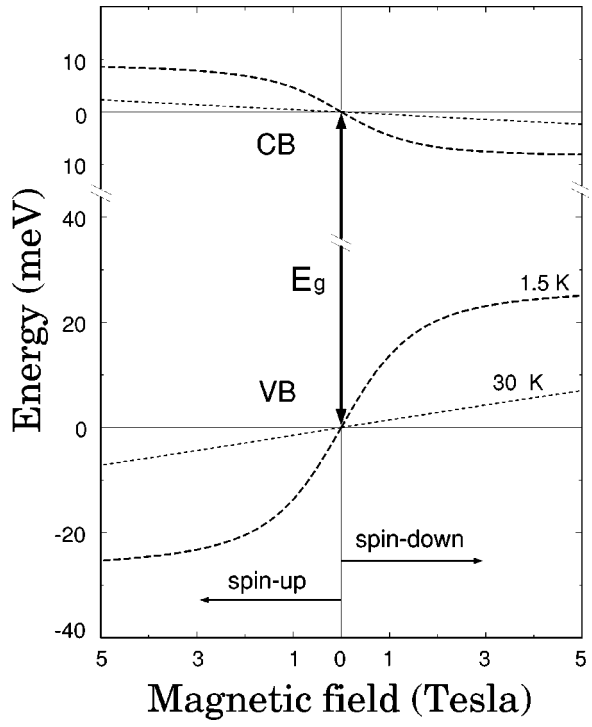

FIG. 4. Calculated band edge splitting of the conduction and the heavy-hole bands in $Zn_{1-y}Mn_ySe$ with $y \approx 0.04$. The regions to the left and to the right of $B=0$ show the behavior of the spin-up and the spin-down band edges, respectively. E_g is the energy gap at $B=0$.

To perform optical transmission experiments on the MQW samples, the GaAs substrate had to be removed. This was done by mechanical polishing, followed by selective chemical etching ($1:20NH_4OH:H_2O_2$) at room temperature. The interband magnetoabsorption experiments were performed in an optical cryostat ($T \geqslant 1.5$ K) equipped with a 6T superconducting magnet. The light source used in the experiments was a halogen lamp together with a 1-m monochromator. The monochromatic light was circularly polarized, so as to allow the identification of transitions between different spin states. The signal was detected by a photomultiplier tube, and was sent to a lock-in amplifier and a computer-controlled analyzer for data storing and processing.

IV. ZEEMAN SPLITTING OF NEARLY RESONANT COUPLED WELLS

The most interesting features of wave-function distributions in symmetric multiple QW's are seen in systems with identical wells, in which eigenstates of each well are in resonance (see Figs. 1 and 2), and thus strongly coupled by interwell interaction. When the structures are in the off-resonant condition, as is the case when well depths or widths are different, interactions between the eigenstates in each well are considerably weaker. The eigenstates of the system will then have approximately the same features as in isolated single QW's comprising the system. Since our primary purpose is to map out wave functions of *coupled* states, we will restrict ourselves to *very small* depth variations of the DMS well (i.e., to small Zeeman splittings). Maintaining the (nearly) resonant condition of the wells in this way results, in the presence of thin interwell barriers, in coupling that is sufficiently strong to resolve transitions involving the lowest multiplet of conduction and valence band states.

As can be seen from Fig. 4, small perturbation of the depth of DMS wells can be achieved either by applying a weak magnetic field at low temperatures, or by strong magnetic fields at higher temperatures. We have chosen to study the high-temperature (30 K) region for the purpose of mapping the wave-function distribution, because the Zeeman shift of DMS band edges shows a relatively linear dependence over a wide field range at that temperature (see Fig. 4), making it easier to follow the Zeeman splitting of the transitions.

A. Triple quantum wells

The most interesting structure for Zeeman mapping of the coupled states in a triple QW is TQW1 (see Fig. 3), because in its DMS well one of the lowest triplet states (the second state) is totally absent (see Fig. 1), making transitions involving that state completely insensitive to the field. The absorption spectra in various magnetic fields taken on TQW1 at 30 K are shown in Fig. 5. These represent excellent examples of the splitting of the degenerate single-well ground state into three states as the three wells become coupled. Even though there actually is a total of six coupled states in TQW1 (three

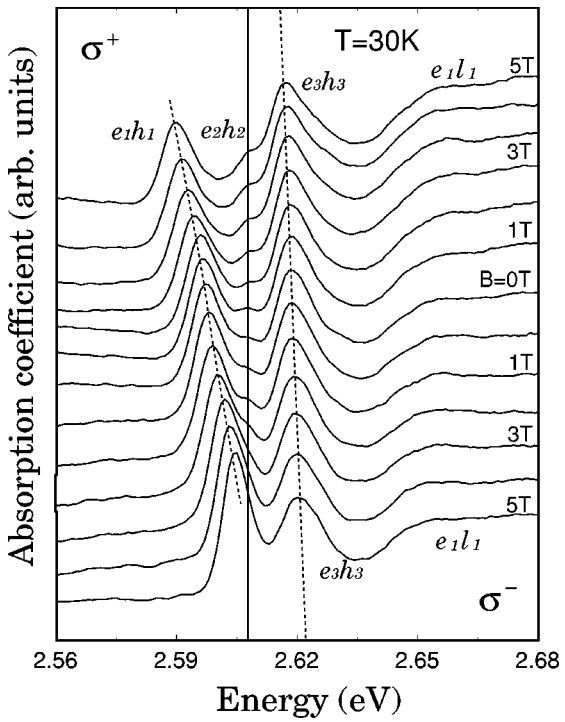

FIG. 5. Absorption spectra taken at 30 K for TQW1 at different magnetic fields. σ^+ and σ^- refer to spin-down and spin-up transitions, respectively. Magnetic field dependence of the observed transitions from the triplet of states in the conduction band to that of the heavy-hole band are clearly shown. The dotted lines through e_1h_1 and e_3h_3 are guides for the eyes. The thin solid line is drawn vertically at constant energy, showing that the position of e_2h_2 through which the line passes is independent of the field.

in the conduction band wells and three in the heavy-hole band wells, as shown in Fig. 1), only three strong transitions are expected due to the $\Delta n=0$ selection rule (see Table I). Guided by this rule, the three left-most peaks in Fig. 5 can be attributed to transitions e_1h_1, e_2h_2, and e_3h_3, respectively, as indicated in the figure. The additional broad peak at 2.65 eV (marked e_1l_1) is associated with the light-hole band. Since—as was already mentioned—in the context of this paper we are not interested in transitions involving light holes, we will not discuss peak e_1l_1 further.

In this triple-QW structure, the Zeeman shift of each eigenstate from its zero-field position is determined by the overlap of the probability $|\Psi|^2$ of that state with the DMS layer. In first order approximation, the shift of the nth eigenstate can be written

$$\Delta E_n^{c,v}=P_n\Delta E^{c,v}, \tag{1}$$

where P_n is the probability density of carriers in the nth eigenstate integrated over the DMS layer, and $\Delta E^{c,v}$ is the Zeeman shift of the conduction (c) or valence (v) band edge of a DMS layer with 4% Mn ions, depending on whether the nth state is in the conduction or the valence band. Thus the observed Zeeman shift of a given transition will indicate where the wave functions of states involved in that transition are located. In Fig. 5 it is clear that the strongest magnetic field dependence is seen for the e_1h_1 transition, and no noticeable energy variation with field is observed for the e_2h_2, as would be expected from the wave-function distributions

TABLE III. Total Zeeman splittings of successive transitions observed at 5 T, and probabilities of the heavy-hole states in the central (DMS) well for TQW1.

	e_1h_1	e_2h_2	e_3h_3		h_1	h_2	h_3
ΔE_n(meV)	14.5	0	3.3	$\lvert\psi_n^v\rvert^2$	0.73	0.01	0.17
$\Delta E_n/\Delta E_1$	1	0	0.228	$\lvert\psi_n^v\rvert^2/\lvert\psi_1^v\rvert^2$	1	0	0.233

shown in Fig. 1. The solid line in Fig. 5 was actually drawn as a straight vertical line at the position of the e_2h_2 transition at zero magnetic field. It is quite striking that this transition appears always at the same energy even in the presence of a magnetic field. This strongly indicates that the e_2 and h_2 states are indeed localized only in the two side wells, which in the case of TQW1 are non-DMS layers.

We now note that the Zeeman shift of the heavy-hole band edge is significantly larger (about four times; see Fig. 4) than that of the conduction band edge. In practice the observed Zeeman shift of the transitions ΔE_n will thus be dominated by the contribution from the heavy-hole band. In Table III we compare the Zeeman splitting between σ^+ and σ^- transition energies observed at 5 T, and the probability density of the heavy-hole states integrated over the central DMS well for TQW1. There is indeed rather good correlation between the ratios of the Zeeman splittings of the various transitions and the ratios of the calculated probability densities in the DMS well of the corresponding heavy-hole states.

Measurements on TQW2 show that all transitions (including e_2h_2) are field dependent. This is as would be expected, since in that case the side wells consist of DMS material, and thus wave functions of *all* states are at least partially localized in the DMS wells, as seen in Fig. 1. Furthermore—in contrast with TQW1—now the shift of the e_2h_2 transition is actually *the greatest*, since states participating in this transition are *entirely* localized in the DMS layers. This feature is indeed clearly observed in magnetoabsorption data for TQW2. The Zeeman splitting between σ^+ and σ^- transition energies observed at 5 T and the probability density of the heavy-hole states integrated over the central DMS well for TQW2 are shown in Table IV. Even though the agreement between the ratios of the Zeeman splittings of the observed transitions and the ratios of the calculated probability densities of the corresponding hole states in the DMS wells is not as good as in the case of TQW1, the comparison gives at least a qualitative understanding of wave-function localization of the states involving the observed transitions.

TABLE IV. Total Zeeman splittings of successive transitions observed at 5 T, and probabilities of the heavy-hole states in the side (DMS) wells for TQW2.

	e_1h_1	e_2h_2	e_3h_3		h_1	h_2	h_3
ΔE_n(meV)	5.6	11.5	[a]	$\lvert\psi_n^v\rvert^2$	0.69	0.87	0.20
$\Delta E_n/\Delta E_1$	1	2.05	[a]	$\lvert\psi_n^v\rvert^2/\lvert\psi_1^v\rvert^2$	1	1.26	0.29

[a] e_3h_3 transition was not observed in TQW2.

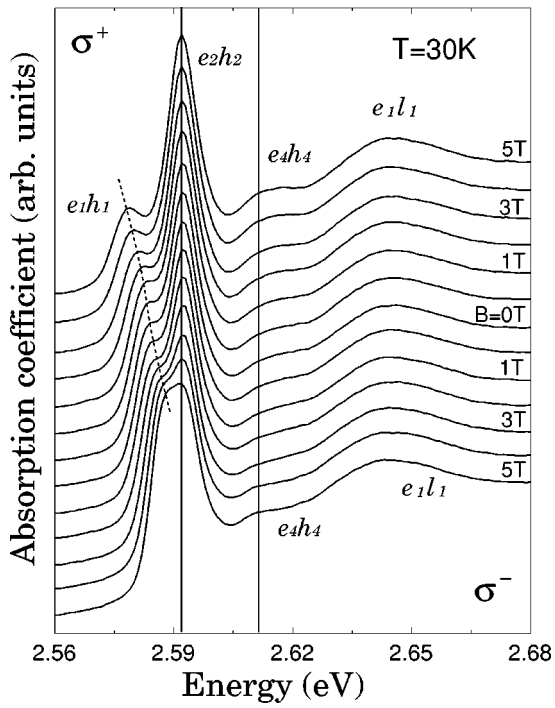

FIG. 6. Absorption spectra taken at 30 K for QQW1 at different magnetic fields. σ^+ and σ^- refer to spin-down and spin-up transitions, respectively. Magnetic field dependence of the observed e_1h_1 transition clearly shown (the dotted line is a guide for the eyes). Solid vertical lines are drawn independent of the field, showing that transitions through which they pass are field independent.

B. Quintuple quantum wells

For wave-function mapping in quintuple quantum wells, both QQW1 and QQW2 shown in Figs. 2 and 3 are suitable structures. We will concentrate on QQW1, since in this structure there are *two* states whose probability is totally absent in the DMS well. Following the splitting of eigenstates in this structure due to interwell coupling, one expects five most probable e_nh_n transitions, for n from 1 to 5. However, it is very hard to observe all of these transitions separately, because the five states involved are closely spaced within a small energy window. In QQW1, three transitions, e_1h_1, e_2h_2, and e_4h_4, are clearly observed in absorption spectra taken at 30 K, as shown in Fig. 6. (The weak and wide peak around 2.65 eV is the transition related to the light-hole band, already pointed out in connection with TQW1.) The magnetic field dependence of these transitions again provides information on the localization of the states involved. The e_1h_1 transition shows a strong dependence on the magnetic field, as in TQW1, indicating the presence of the wave function in the central well, which is a DMS layer. The most revealing feature shown by QQW1 is the lack of field dependence of the e_2h_2 and e_4h_4 transitions. The solid lines drawn at the positions of e_2h_2 and e_4h_4 transitions in Fig. 6 are straight in vertical direction, independent of the field. This is a beautiful example of Zeeman mapping of wave-function distributions in multiple quantum wells, since-as is clearly seen in Fig. 2-the states involved in these transitions have a ''blind spot'' in the central (DMS) well. Although it is difficult to see all quintuple-well transitions, we note that the e_4h_4 line is quite broad, and changes shape with field, indicating that other (weak) lines may be present in its vicinity. Unfortunately the resolution of the data is insufficient to warrant further discussion of this point.

The results observed on QQW2 differ only in detail, bearing out the ability of this approach to determine where the states of the ground-state multiplet are localized. Thus in contrast to QQW1, transitions e_1h_1 and e_2h_2 observed for QQW2 show magnetic shift, while the e_3h_3 transition does not show magnetic shift.

V. SUMMARY

We investigated symmetric multiple (triple and quintuple) arrays of QW's using magnetoabsorption experiments. Since we are interested in the wave-function distribution of the coupled states in these systems, we grew the multiple QW's using strategically chosen combinations of DMS and non-DMS layers. Specifically, $Zn_{1-x}Cd_xSe$ and $Zn_{1-x-y}Cd_xMn_ySe$ were used for the well layers, and ZnSe was used for the barriers. In triple QW's (TQW1 and TQW2), we observed three transitions involving the lowest triplet of eigenstates in the conduction and the heavy-hole band. From their behavior in magnetic field, we were able to qualitatively describe the wave-function distributions of these states under the condition of strong (resonant) coupling. In particular, by observing almost no Zeeman splitting of the e_2h_2 transition in TQW1, and the largest Zeeman splitting of that same transition in TQW2, it was confirmed that the second-lowest states (e_2 and h_2) are localized exclusively in the side wells of the system.

We were not able to observe all transitions from the lowest quintuplet of states in the quintuple QW's. It is in fact remarkable that we can resolve most of the individual transitions separately in what already approaches a *superlattice* subband. The observed transitions in QQW1 and QQW2 also show interesting magnetic behavior, indicating the localization of individual wave functions involved in the transitions—and, particularly, their *absence* in certain wells of the MQW structures.

It should be noted that the intensity of the transitions changes significantly with magnetic field in all multiple QW's investigated. This cannot be explained simply by the wave-function overlap arguments. Since all transitions involving the multiplet of states *originate from the ground state of a single QW*, intensities are expected to be correlated (i.e., not independent of one another). Such a correlation phenomenon was already clearly observed in the case of DQW's, and was understood in terms of an intensity sum rule involving coupled-state transitions.[19] To extend the details of this concept to the much more complex situation of multiple QW's is beyond the scope of this study, but should constitute an important goal of a future investigation.

ACKNOWLEDGMENTS

The authors are grateful to H. Luo and G. Yang for many fruitful discussions. This work was supported by NSF Grant No. DMR 97-05064.

[1] R. Dingle, A.C. Gossard, and W. Wiegmann, Phys. Rev. Lett. **34**, 1327 (1975).
[2] C. Delalande, U.O. Ziemelis, G. Bastard, M. Voos, A.C. Gossard, and W. Wiegmann, Surf. Sci. **142**, 498 (1984).
[3] H.Q. Le, J.J. Zayhowski, and W.D. Goodhue, Appl. Phys. Lett. **50**, 1518 (1987).
[4] Y.J. Chen, E.S. Koteles, B.S. Elman, and C.A. Armiento, Phys. Rev. B **36**, 4562 (1987).
[5] S. Tarucha, K. Ploog, and K. Von Klitzing, Phys. Rev. B **36**, 4558 (1990).
[6] K. Leo, J. Shah, O. Göbel, T.C. Damen, S. Schmitt-Rink, and W. Schäfer, Phys. Rev. Lett. **66**, 201 (1991).
[7] P. Yuh and K.L. Wang, Phys. Rev. B **38**, 8377 (1988).
[8] J. Cen and K.K. Bajai, Phys. Rev. B **46**, 15 280 (1992).
[9] N. Debbar, S. Hong, J. Singh, P. Bhattacharya, and R. Sahai, J. Appl. Phys. **65**, 383 (1988).
[10] A. Yariv, C. Lindsey, and Uri Sivan, J. Appl. Phys. **58**, 3669 (1985).
[11] H. Kawai, K. Kaneko, and N. Watanabe, J. Appl. Phys. **58**, 1263 (1975).
[12] T. Kamizato and M. Matsuura, Phys. Rev. B **40**, 8378 (1989).
[13] J.F. Smyth, D.D. Awschalom, N. Samarth, H. Luo, and J.K. Furdyna, Phys. Rev. B **46**, 4340 (1992).
[14] T. Tanoue, H. Mizuta, and S. Takahashi, IEEE Electron Device Lett. **9**, 365 (1988).
[15] D.A. Collins, D.H. Chow, D.Z.Y. Ting, E.T. Yu, J.R. Söderström, and T.C. McGill, Solid-State Electron. **32**, 1095 (1989).
[16] C. Juang, R.Y. Hwang, H.C. Pan, C.M. Chang, and B.J. Lee, J. Appl. Phys. **70**, 4973 (1991).
[17] S. Fukuta, H. Goto, N. Sawaki, T. Suzuki, H. Ito, and K. Hara, Semicond. Sci. Technol. **8**, 1881 (1993).
[18] T. Kai, M. Morifuji, M. Yamaguchi, and C. Hamaguchi, Semicond. Sci. Technol. **9**, 1465 (1994).
[19] S. Lee, M. Dobrowolska, J.K. Furdyna, H. Luo, and L.R. Ram-Mohan, Phys. Rev. B **54**, 16 939 (1996).
[20] L.R. Ram-Mohan, S. Saigal, D. Dossa, and J. Shertzer, Comput. Phys. **4**, 50 (1990).
[21] M.M. Dignam and J.E. Sipe, Phys. Rev. B **43**, 4084 (1991).
[22] P. Bonnel, P. Lefebvre, B. Gil, H. Mathieu, C. Deparis, J. Massies, G. Neu, and Y. Chen, Phys. Rev. B **42**, 3435 (1990).
[23] B. Deveaud, A. Chomette, F. Clerot, P. Auvray, A. Regreny, R. Ferreira, and G. Bastard, Phys. Rev. B **42**, 7021 (1990).
[24] F.C. Zhang, N. Dai, H. Luo, N. Samarth, M. Dobrowolska, J.K. Furdyna, and L.R. Ram-Mohan, Phys. Rev. Lett. **68**, 3220 (1991).
[25] F.C. Zhang, H. Luo, N. Dai, N. Samarth, M. Dobrowolska, and J.K. Furdyna, Phys. Rev. B **47**, 3806 (1993).
[26] H. Luo, W.C. Chou, N. Samarth, A. Petrou, and J.K. Furdyna, Solid State Commun. **85**, 691 (1993).
[27] H. Luo, N. Dai, F.C. Zhang, N. Samarth, M. Dobrowolska, J.K. Furdyna, C. Parks, and A.K. Ramdas, Phys. Rev. Lett. **70**, 1307 (1993).
[28] J. A. Gaj, C. Bodin-Deshayes, P. Peyla, J. Cibert, G. Feuillet, Y. Merle d'Aubigne, R. Romestain, and A. Wasiela, in *Proceedings of the 21st International Conference on the Physics of Semiconductors*, edited by P. Jiang and H.-Z. Zheng (World Scientific, Singapore, 1992), p. 1936.
[29] N. Dai, L.R. Ram-Mohan, H. Luo, G.L. Yang, F.C. Zhang, M. Dobrowolska, and J.K. Furdyna, Phys. Rev. B **50**, 18 153 (1994).